77. THE PHYSICAL STATE OF THE UPPER LEVELS OF CRETACEOUS OCEANIC CRUST FROM THE RESULTS OF LOGGING, LABORATORY STUDIES, AND THE OBLIQUE SEISMIC EXPERIMENT AT DEEP SEA DRILLING PROJECT SITES 417 AND 418

Matthew H. Salisbury,[1] Ralph Stephen,[2] Nikolas I. Christensen,[3]
Jean Francheteau,[4] Yozo Hamano,[5] Michael Hobart,[6] and Douglas Johnson[7]

ABSTRACT

The combined results of logging, physical properties studies, and the oblique seismic experiment conducted during DSDP Legs 51 through 53 at Sites 417 and 418 in Cretaceous crust at the southern end of the Bermuda Rise make possible the first detailed evaluation of the physical state of the upper levels of old oceanic crust.

From an analysis of the results of the oblique seismic experiment, it appears that the *P*-wave velocity increases linearly from 4.8 ±0.2 km/s at the top of Layer 2 to 6.4 ±0.2 km/s at a sub-basement depth of 1.3 km. The *P*-wave velocity of Layer 3 at approximately 1.5 km is 6.7 ±0.2 km/s. The *S*-wave velocity is 2.6 ±0.1 km/s at the top of Layer 2 and 3.7 ±0.1 km/s at the top of Layer 3.

The average value of V_P (4.8 km/s) measured by logging in the uppermost basement in Hole 417D is in excellent agreement with the value obtained from the oblique seismic experiment, but is lower than the formation velocity (5.3 to 5.6 km/s) reconstructed for the site from laboratory measurements of velocity through recovered core material. This requires that the formation contains cracks on a scale finer than the resolution of the logging and oblique seismic experiments, but greater than that of laboratory samples. On the basis of these results and petrologic constraints imposed by the core, the upper crust in Hole 417D consists of 90 per cent basalt with an average grain boundary porosity of 8 per cent, less than 1 per cent interpillow limestone, 5 per cent smectite consisting of about 50 per cent water, and 5 per cent open cracks filled with standing water. The formation porosity thus resides in two domains, grain boundaries and open cracks, and totals 13 to 14 per cent. This value is confirmed by electrical resistivity logs which indicate, in addition, that the cracks are interconnected, giving the formation an average permeability in the thousands of darcies, with lower values in the less fractured massive basalts.

Comparison of these results with logging data obtained in young crust in Hole 396B on the Mid-Atlantic Ridge indicates that, although the porosity and permeability of the upper levels of the crust at Site 417 are much lower than at the ridge crest, the formation is not entirely sealed. Although water circulation is thus still possible in old crust, it may be limited by the presence of massive basalts and the absence of shallow sources of heat.

[1]Deep Sea Drilling Project and Geological Research Division, Scripps Institution of Oceanography, University of California, San Diego, La Jolla, California.

[2]Department of Geodesy and Geophysics, University of Cambridge, Cambridge, England (now at the Department of Geology and Geophysics, Woods Hole Oceanographic Institution, Woods Hole, Massachusetts).

[3]Department of Geological Sciences and Graduate Program in Geophysics, University of Washington, Seattle, Washington.

[4]Centre Océanologique de Bretagne, Brest, France.

[5]Geophysical Institute, University of Tokyo, Tokyo, Japan.

[6]Lamont-Doherty Geological Observatory, Palisades, New York.

[7]Program in Geosciences, University of Texas at Dallas, Richardson, Texas (now at the Graduate Program in Geophysics, University of Washington, Seattle, Washington).

INTRODUCTION

During the past several decades, our perception of the structure of the oceanic crust (Table 1) has evolved from simple layered models derived from surface refraction data (e.g., Raitt, 1963), through multiple layered models based on ocean bottom seismometer and sonobuoy data (e.g., Hussong, 1972; Peterson et al., 1974; Houtz and Ewing, 1976), to detailed velocity gradient models derived from velocity and amplitude analysis of reflection and refraction data (e.g., Helmberger and Morris, 1970; Orcutt et al., 1976; Spudich et al., 1978). Although the velocity structure of the crust can now be determined in considerable detail,

TABLE 1
Models of Oceanic Seismic Structure

Three-Layer Model[a]			Multiple Layer Model[b,c]		
Layer	Velocity V_P (km/s)	Thickness (km)	Layer	Velocity V_P (km/s)	Thickness (km)
1	~2.0	~0.5	1	1.7-2.0	0.5
2	5.07 ±0.63	1.71 ±0.75	2A	2.5-3.8	0.5-1.5
			2B	4.0-6.0	0.5-1.5
3	6.69 ±0.26	4.86 ±1.42	3A	6.5-6.8	2.0-3.0
			3B	7.0-7.7	2.0-5.0
Mantle	8.13 ±0.24	–	Mantle	8.1	–

[a]After Raitt, 1963.
[b]After Peterson et al., 1974.
[c]Houtz and Ewing (1976) have proposed dividing Layer 2 into Layers 2A, B, and C having average velocities of 3.64, 5.19, and 6.09 km/s, respectively.

its composition has remained largely conjectural beyond the limits of direct sampling. This is because of the difficulties of interpreting velocities in terms of petrology in the absence of *in situ* data on the distribution of cracks and voids in the basement and their effects upon *in situ* pressure, water saturation, and formation velocity.

During the past five years, several attempts have been made to drill deep into the oceanic basement to determine its petrology and geophysical behavior directly. Although the composition of the crust is known from such efforts to depths of more than 0.5 km at several sites in the Atlantic (Table 2), low core recovery has prevented reconstruction of its geophysical behavior.

Recently, two attempts have been made to measure the *in situ* physical properties of the crust by means of downhole geophysical experiments. During the first such experiment (Kirkpatrick, 1978), a 200-meter section of basement was logged in Hole 396B in 10-m.y.-old crust at 23°N on the Mid-Atlantic Ridge. Although the operating conditions were not perfect, the experiment nonetheless clearly demonstrated that *in situ* compressional wave velocities in young crust are consistent with those of Layer 2A (Houtz and Ewing, 1976) and that the porosity and fluid permeability of the uppermost levels of the basement are extremely high owing to the presence of numerous water-filled cracks and voids.

The second attempt, consisting of both downhole logging and the first successful application of the oblique seismic experiment (Stephen et al., this volume), was recently completed in Hole 417D in conjunction with drilling conducted in 108-m.y.-old crust at the southern end of the Bermuda Rise during Legs 51 through 53 (Figure 1). As can be seen in Figure 2 and Table 3, four holes were drilled during this program for a cumulative basement penetration of 1129 meters and a maximum penetration in one hole (Hole 418A) of 544 meters. The results of laboratory studies of the rocks obtained from these holes (Site 417 and 418 Reports; Christensen et al.; Hamano; Johnson; all, this volume), together with those of the downhole logging and oblique seismic experiments in Hole 417D (Salisbury et al.; Stephen et al.; both, this volume), represent the most comprehensive body of geophysical data in existence on the *in situ* properties of the crust. The purpose of the present paper is to determine the physical state of Layer 2 from a review of these data and from a comparison of results determined at different scales of investigation in the same hole.

BASEMENT LITHOLOGY AND PHYSICAL PROPERTIES

The section drilled at Sites 417 and 418 consists of approximately 300 meters of unconsolidated-to-semi-consolidated pelagic clay, claystone, and chalk of Recent to early Aptian age underlain by pillow basalt, breccia, and massive basalt; the massive basalt is cut by dikes in the bottom of the deepest holes (Holes 417D and 418A). The basalts are plagioclase-phyric with subordinate phenocrysts of olivine ± clinopyroxene and tend to fairly uniform in composition.

TABLE 2
Deep Basement Penetration Sites in the Atlantic

Leg	Hole	Location	Basement Penetration (m)	Recovery in Basement (%)	Age (m.y.)	Downhole Experiments
37	332A[a]	36°52.72'N, 33°38.46'W	230	10	3.5	
37	332B[a]	36°52.72'N, 33°38.46'W	589	21	3.5	
37	333A[b]	36°50.45'N, 33°40.05'W	300	8	3.5	
45	395A[c]	22°45.35'N, 46°04.90'W	580	18	7	
46	396B[d]	22°59.14'N, 43°30.90'W	256	23	10	Logging[e]
49	409[f]	62°36.98'N, 25°57.17'W	240	24	2.3	
51 through 53	417A[g]	25°06.63'N, 68°02.48'W	209	61	108	
51 through 53	417D[g]	25°06.69'N, 68°02.82'W	366	72	108	Logging[h], Oblique Seismic Exp.[i]
51 through 53	418A[j]	25°02.10'N, 68°03.44'W	544	72	108	

[a]Site 332 Report *in* Aumento, Melson, et al., 1977a.
[b]Site 333 Report *in* Aumento, Melson, et al., 1977b.
[c]Site 395 Report *in* Melson, Rabinowitz, et al., 1979.
[d]Site 396 Report *in* Dmitriev, Heirtzler, et al., 1979.
[e]Kirkpatrick, 1978.
[f]Site 409 Report *in* Cann, Luyendyk, et al., 1979.
[g]Site 417 Report (this volume).
[h]Salisbury et al. (this volume).
[i]Stephen et al. (this volume).
[j]Site 418 Report (this volume).

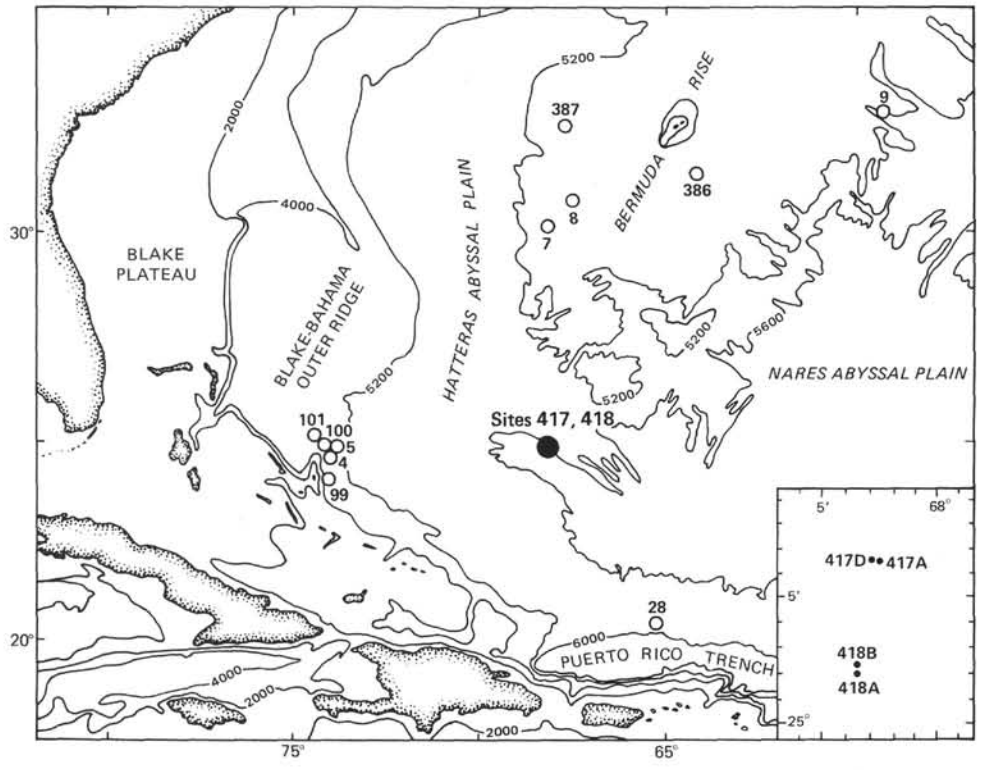

Figure 1. *Location of DSDP Holes 417A, 417D, 418A, and 418B. Oblique seismic and logging experiments were conducted in Hole 417D.*

Despite their age, they are fresh with the exception of those recovered from the upper levels of Hole 417A, which are among the most profoundly altered basalts ever recovered from the sea floor (Donnelly et al., this volume). Since the basal Aptian to Cenomanian section is missing in Hole 417A (Figure 2) and the hole was drilled into a small basement high, it has been suggested that the basement section in the hole had been exposed to sea water for millions of years before its eventual burial (Site 417 Report, this volume).

As can be seen in Table 3, the basement material recovered at Sites 417 and 418 consists of 71 per cent pillow basalt, 22 per cent massive basalt, and 7 per cent breccia. Of this material, about 6 per cent consists of smectite and calcite fillings in cracks and between pillows. Although studies of the distribution of cracks in the core (Johnson, this volume) indicate that the basement may be strongly fractured *in situ*, the recovery at Sites 417 and 418 was unusually high (70%), owing to partial healing of the crust by such material. This suggests that the figures cited in Table 3 are representative of the drilled section, and thus of the upper levels of Layer 2 in old crust.

Detailed studies of the physical properties of the material recovered from these holes have been made by several investigators and are reported elsewhere (Site 417 and 418 Reports; Christensen et al.; Hamano; Johnson; all, this volume). These include measurements at room temperature and pressure of wet-bulk density, porosity, compressional and shear wave velocity, permeability, thermal conductivity, and electrical resistivity as well as measurements of compressional wave velocity as a function of hydrostatic confining pressure. The wet-bulk density, porosity, and compressional wave velocity data obtained at room temperature and pressure from these studies, together with calculated values of grain density and acoustic impedance, are shown as a function of depth for Holes 417A and 417D in Figures 3 and 4, respectively, and for Holes 418A and 418B in Figure 5. Also shown are synthetic physical property profiles for each hole based on the values shown and section-by-section estimates of the relative abundance of basalt, smectite, and calcite. The density profile was reconstructed from the relation,

$$\rho_s = x_b \rho_b + x_{sm} \rho_{sm} + x_{ls} \rho_{ls} \quad (1)$$

where ρ_s is the mean density of the depth interval or section under consideration; x_b, x_{sm}, and x_{ls} are the respective volumetric fractions of basalt, smectite, and limestone in the interval; ρ_b is the nearest measured density value in basalt; ρ_{sm} is the mean density of smectite in the hole (2.20 g/cm^3, 2.40 g/cm^3, and 2.45 g/cm^3 in Holes 417A, 417D, and both Holes 418A and 418B, respectively), and ρ_{ls} is the density of limestone (2.7 g/cm^3).

Similarly, the velocity, impedance, and porosity profiles were determined as a function of depth from the relations,

$$V_{p_s} = \left[\frac{x_b}{V_{p_b}} + \frac{x_{sm}}{V_{p_{sm}}} + \frac{x_{ls}}{V_{p_{ls}}}\right]^{-1} \quad (2)$$

$$Z_s = (V_{p_s})(p_s) \quad (3)$$

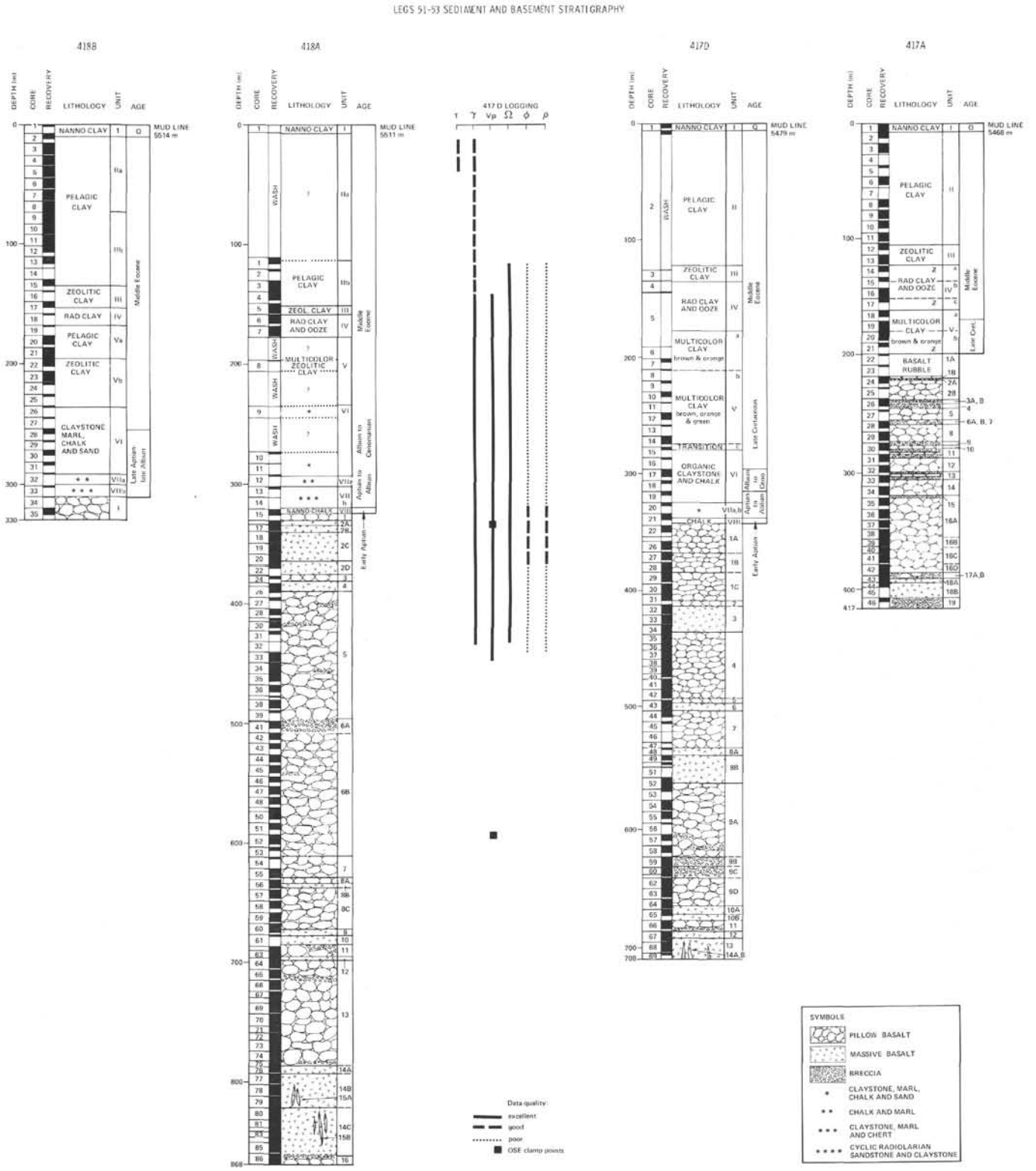

Figure 2. *Lithology versus depth in Holes 417A, 417D, 418A, and 418B. Also shown are estimates of the quality of the logging data and the positions of the geophone during the oblique seismic experiment in Hole 417D.* γ, V_p, Ω, ϕ, *and* ρ *stand for the natural gamma ray, velocity, resistivity, porosity, and density logs, respectively.*

TABLE 3
Basement Lithology at Sites 417 and 418[a]

Hole	Drilled (m)	Recovered (%)	Recovered Lithology: Pillow Basalt (%)	Massive Basalt (%)	Breccia (%)
417A	209.0	61	75	9	16
417D	365.5	72	71	24	5
418A	544.0	72	69	27	4
418B	10.1	74	100	0	0
Total	1128.6	70	71	22	7

[a] Site 417 and 418 Reports (this volume).

and

$$\phi_s = x_b\phi_b + x_{sm}\phi_{sm} + x_{ls}\phi_{ls} . \quad (4)$$

where V_{Ps}, V_{Pb}, V_{Psm}, and V_{Pls} are, respectively, the compressional wave velocity of the section in question, the nearest measured velocity value in basalt, the mean smectite velocity in the hole (2.9 km/s, 3.8 km/s, and 4.0 km/s in Holes 417A, 417D, and both Holes 418A and 418B, respectively), and the velocity of limestone (5.9 km/s); Z_s is the acoustic impedance of the interval; and ϕ_s, ϕ_b, ϕ_{sm}, and ϕ_{ls} are, respectively, the porosity of the section, the nearest measured porosity value in basalt, the mean porosity of smectite in the hole (54% in Holes 417A and 417D, and 20% in Holes 418A and 418B), and the porosity of limestone (equated to that of the nearest basalt). The profiles shown were calculated on a section-by-section basis, that is, in 1.5-meter-long increments roughly equivalent to the sensor spacing in downhole logging tools. Since for the purposes of calculation the formation was considered to be crack-free, the synthetic velocities, densities, and impedances shown are maximum values, and the porosities are minimum values.

A comparison between these profiles and the laboratory measurements upon which they are based shows that the density and velocity measurements do not represent formation properties but rather maximum density and velocity envelopes for each hole, while the porosity values represent minimum envelopes. The discrepancy is largely due to sampling bias: although care was taken to sample each component (basalt, smectite, or limestone) according to its overall abundance in the core, this was often impractical within specific lithologic units. Consequently, the physical properties of the smectites are often inadequately represented in the laboratory data. This discrepancy can be substantial, particularly in zones of strong alteration. For example, the synthetic velocities of lithologic Units 4, 9, and 13 in Hole 417A are considerably lower than the laboratory velocities of the relatively unaltered samples actually examined in their vicinity. Since the synthetic profiles are based on laboratory data but reduce the effects of sampling bias, they are considered to represent the data more realistically.

It is clear in Figures 3, 4, and 5 that many (but not all) of the units distinguished on lithologic grounds can also be delineated on the basis of physical properties. For example, in Hole 417A, Units 1 and 2 can be clearly distinguished from Units 3 and 4, 5 through 8, 9 through 11, 12, 13, 14 through 18, and 19; while in Hole 417D, Units 1 and 2 can be distinguished from Units 3, 4, 5 through 9b, 9c, 9d through 11, and 12 through 14; and in Hole 418A, Units 1 through 4 can be distinguished from Units 5 through 6a and 6b through 16. Among these subdivisions, the breccias are notable for their high smectite content (locally greater than 50% by volume) and consequently high porosity, low density, and low velocity, while the massive basalts display low porosities, high densities, and high velocities beneath a strongly altered, low-velocity cap formed by prolonged interaction with sea water at elevated temperatures. Not unexpectedly, the physical properties of the pillow basalts tend to range irregularly between these two extremes. Although the units described above can be distinguished in terms of physical properties, it is unlikely that many can be detected geophysically. The only likely exceptions are the breccias, which may be detectable as sub-basement reflectors because of their low acoustic impedances.

From the physical properties data summarized in Table 4, it is clear that there is a pronounced difference between basalts recovered from holes drilled in topographic depressions (Holes 417D and 418A) and basalts from topographic highs (Hole 417A). The compressional wave velocities and wet-bulk densities of samples from Holes 417D and 418A, for example, average 5.5 km/s and 2.8 g/cm^3, respectively, while the porosities average 8.4 per cent. These values are in marked contrast to those observed in Hole 417A, which average 5.0 km/s, 2.7 g/cm^3, and 13.7 per cent, respectively. Since the age and lithology of the holes are virtually identical, the differences in physical properties are attributed to differences in alteration due to varying exposure to sea water. Such an explanation is consistent with the presence of sharp physical properties gradients in the upper levels of Hole 417A. If this conclusion is correct, it is clear from the more subtle, but no less striking, gradients in Hole 418A (Figure 5), that the effects of alteration are noticeable to considerable depths in the crust. A projection of the laboratory data, for example, suggests that the porosity approaches zero and the wet-bulk density approaches the grain density (i.e., the physical properties approach intrinsic values) at about 700 meters sub-basement.

Although of considerable interest, it must be borne in mind that the physical properties discussed thus far were measured on small samples that were free of large cracks. Since the velocities of fresh basalts measured in the laboratory tend to be considerably higher than those observed for the upper levels of Layer 2, it is clear that at least the upper levels of the crust are strongly fractured. To understand the significance of such cracks, we must examine data obtained on a larger scale of investigation.

DOWNHOLE LOGGING IN HOLE 417D

As can be seen in Figure 2, an extensive program of downhole geophysical logging was conducted in Hole 417D in an effort to obtain *in situ* data on the physical properties of both the sediment column and the underlying basement. Although the uppermost levels of the sediments could not be logged directly (the hole was cased by drill pipe to a depth of 114 m and, later, to 144 m, to prevent caving), the open

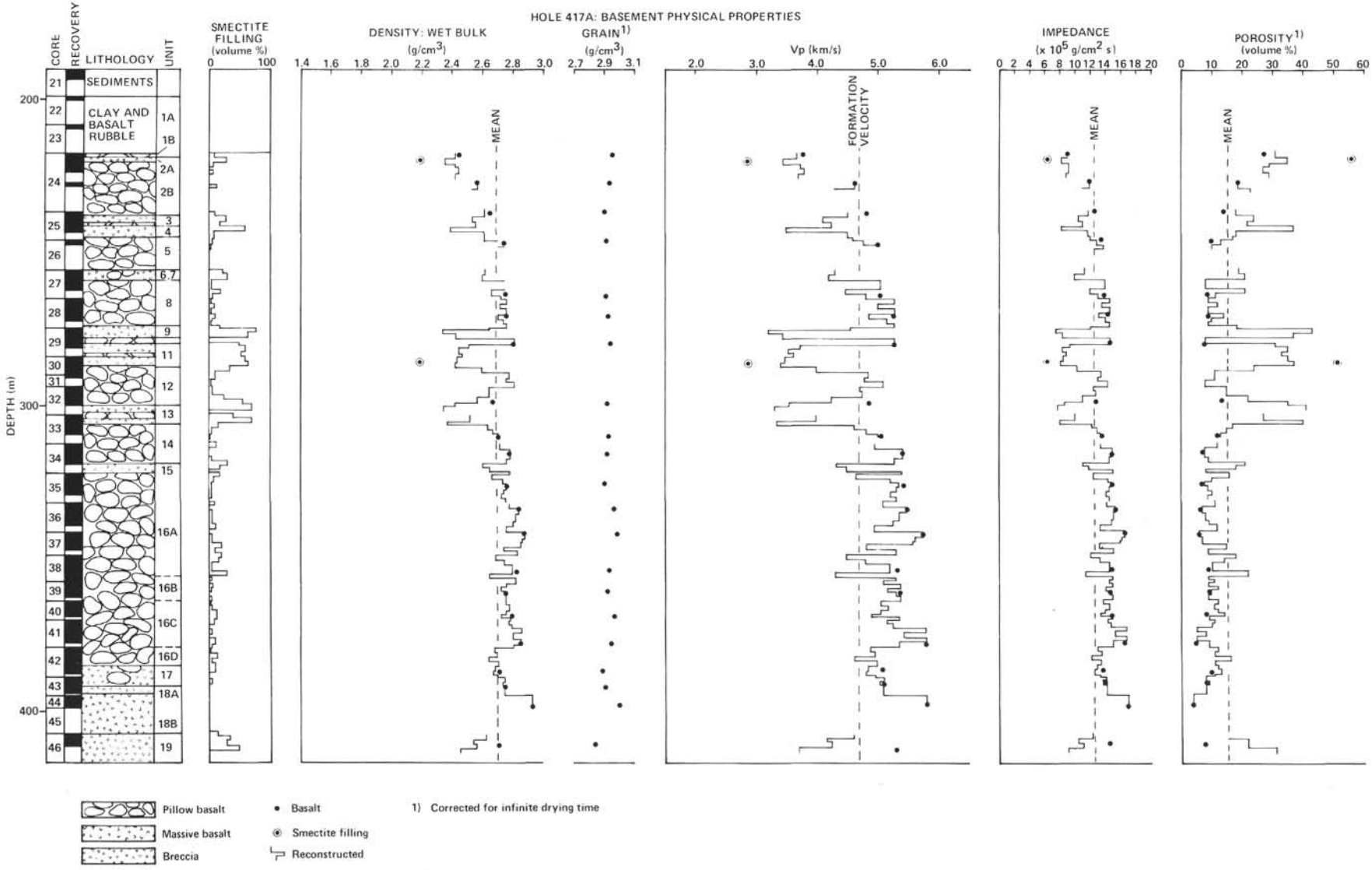

Figure 3. *Lithology, interstitial fillings, and physical properties versus depth in Hole 417A. Synthetic profiles based on laboratory measurements and estimates of the relative abundance of basalt, smectite, and calcite in each section (see text).*

hole below the pipe was logged in four stages to an obstruction in the basement at 445 meters sub-bottom using Schlumberger high-resolution temperature, natural gamma ray, density, porosity, velocity, resistivity, and caliper tools in various combinations (Table 5). In addition, the uppermost sediments were logged through the pipe using the natural gamma ray and temperature tools. Results of this experiment, together with a discussion of the tools and their limitations, are presented in detail elsewhere (Salisbury et al., this volume). We will discuss here only the results from the basement section, logged between 343 and 445 meters sub-bottom.

Since many of the properties measured by logging are sensitive to temperature, pressure, hole diameter, and the properties of the fluid in the hole, the data obtained were corrected to *in situ* conditions, assuming a 10-inch hole filled with sea water, an average hydrostatic confining pressure of 0.6 kbar, a temperature at the mudline of 2.4°C (from the temperature log), a temperature gradient of 5.4×10^{-2}C°/m in the sediments (also from the temperature log) and thus, a gradient of 2.2×10^{-2}C°/m in the basalts (as required by uniform heat flow), and a temperature of about 21°C at the top of Layer 2. The corrected logging data for the basement, together with the lithology of the drilled section and visual estimates of the relative abundance of smectite and calcite, are presented in Figure 6.

Although the basalts in Hole 417D have all essentially the same composition, Figure 6 clearly shows that most of the units and subdivisions delineated on the basis of lithology can also be distinguished on the basis of logging. The massive basalts of Unit 3, for example, have distinctly higher and more uniform velocities than the pillow basalts of Units 1, 2, and 4. Individual flows within the pillow basalts can often be distinguished by a sharp decrease in density, resistivity, and velocity, and by a marked increase in porosity and natural gamma-ray activity associated with brecciation, alteration, and potassium enrichment along their contacts (Donnelly et al., this volume).

For the present purpose, however, the most important application of the basement logs is the determination of the *in situ* physical properties of the crust for comparison with laboratory data and with geophysical data obtained from the surface. Since there appears to be no formation damage (the Laterolog 8 and ILD data coincide throughout most of the basement), this can be accomplished provided the logging data can be used quantitatively.

Of the four active tools employed in Hole 417D, the resistivity and velocity tools functioned properly while the density and porosity tools malfunctioned intermittently because of a broken excentralizer. Thus, the resistivity and velocity data are considered to be of high quality throughout the logged section of the hole, while the density and porosity data are considered marginal between 343 and 369 meters sub-bottom and useless below 369 meters, with the possible exception of the low-porosity values observed in Unit 3 between 425 and 433 meters sub-bottom when the tool swung intermittently against the side of the hole.

As can be seen in Figure 6, the electrical resistivity of the uppermost levels of the basement in Hole 417D ranges for the most part between 30 and 80 ohm-meters, with lower values (3 ohm-m) observed in breccias and higher values (up to 200 ohm-m) in massive basalts. Since these *in situ* values are lower than the average laboratory value of electrical resistivity for water-saturated basalts from this interval (97 ohm-m; see Table 7) and markedly lower than the resistivities (10^3 to 10^6 ohm-m) reported by Hyndman and Ade-Hall (1974) for dry basalts at room temperature, it is clear that the basement in Hole 417D is cracked and that the cracks must be filled with sea water (0.25 ohm-m).

Turning to the velocity data, it is apparent in Figure 6 that the compressional wave velocities in the hole range for the most part between 4.7 km/s and 5.3 km/s, with lower velocities displayed in breccias and higher velocities (up to 5.85 km/s) in massive basalts, while the formation velocity derived from integrated transit time data for the entire logged basement interval is 4.8 km/s (Salisbury et al., this volume). Although under certain circumstances there may be a small systematic error in data obtained using the Schlumberger BHC velocity tool (Wang and Simmons, 1978; S. Raymer, personal communication), we see no compelling reason to question the accuracy of the present data. In fact, the logging velocities measured in relatively unfractured sections of the hole (for example, the massive basalts between 424 and 433 m sub-bottom) are indistinguishable from the laboratory velocities of samples from this interval measured at an effective confining pressure appropriate to *in situ* conditions (0.1 kbar).

Interpretation of the porosity data, however, is more difficult. Taken at face value, the porosity logs that were run between 343 and 369 meters before the excentralizer broke suggest that the porosity in the upper part of the hole ranges between 15 and 35 per cent, with an average of 21 to 22 per cent. The minimum value recorded as the tool swung against the side of the hole in the 425- to 433-meter section noted above was 10 per cent. Since the basalts in this interval have a measured porosity of 3 per cent, it is apparent that the logging porosity must be corrected by approximately −7 per cent. As demonstrated by Salisbury et al. (this volume), the correction may be derived independently by comparing the velocity versus density data obtained by logging to corresponding laboratory data obtained at 0.1 kbar for rock samples from the same interval. A density correction of +0.1 g/cm³ is necessary to superimpose the two sets of data. The porosity correction is then the decrease in porosity necessary to restore the porosity versus (corrected) density curve obtained by logging to the porosity-grain density solution observed in the laboratory. The porosity correction thus obtained (−8%) agrees well with that determined above (−7%) and suggests that Unit 1A has an average porosity of 13 to 14 per cent, while Unit 3 has a porosity of about 3 per cent. By the same token, if the density data shown in Figure 6 are corrected by +0.1 g/cm³, it is apparent that Unit 1A has an average density of about 2.7 g/cm³.

Since the velocity and density values obtained in the laboratory are higher than those obtained by logging, while the laboratory porosities are lower, it is obvious that a comparison of the data may be used to estimate the crack porosity and, perhaps, the permeability of the upper levels of the crust. Before attempting such a comparison, however, the results of the oblique seismic experiment will be reviewed to determine the behavior of the crust in the vicinity of Sites

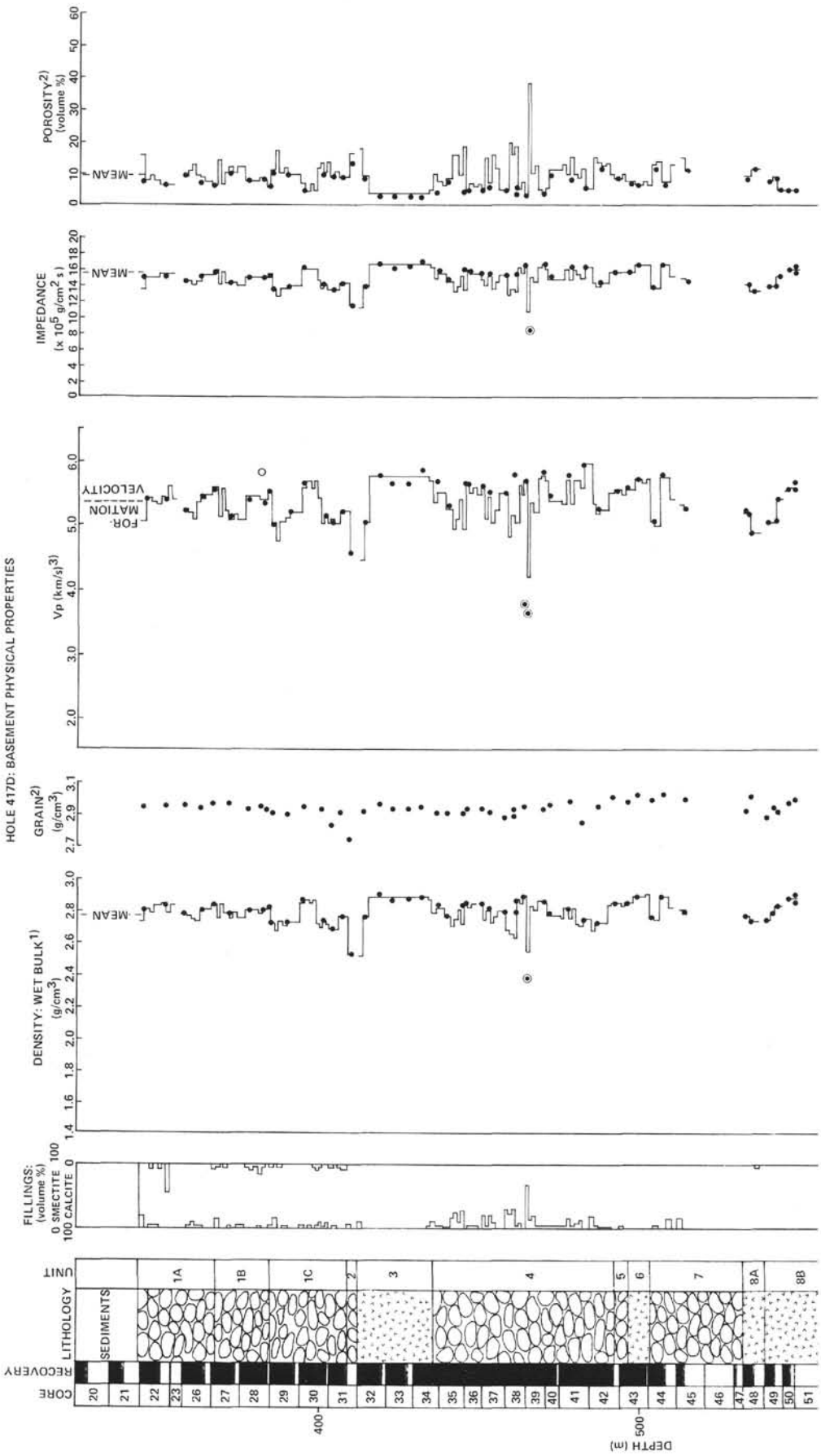
HOLE 417D: BASEMENT PHYSICAL PROPERTIES
POROSITY[2] (volume %)
MEAN
IMPEDANCE (x 10^5 g/cm^2 s)
Vp (km/s)[3]
FOR. MATION VELOCITY
GRAIN[2] (g/cm^3)
DENSITY: WET BULK[1] (g/cm^3)
FILLINGS: (volume %)
SMECTITE
CALCITE
UNIT
LITHOLOGY
SEDIMENTS
RECOVERY
CORE
DEPTH (m)

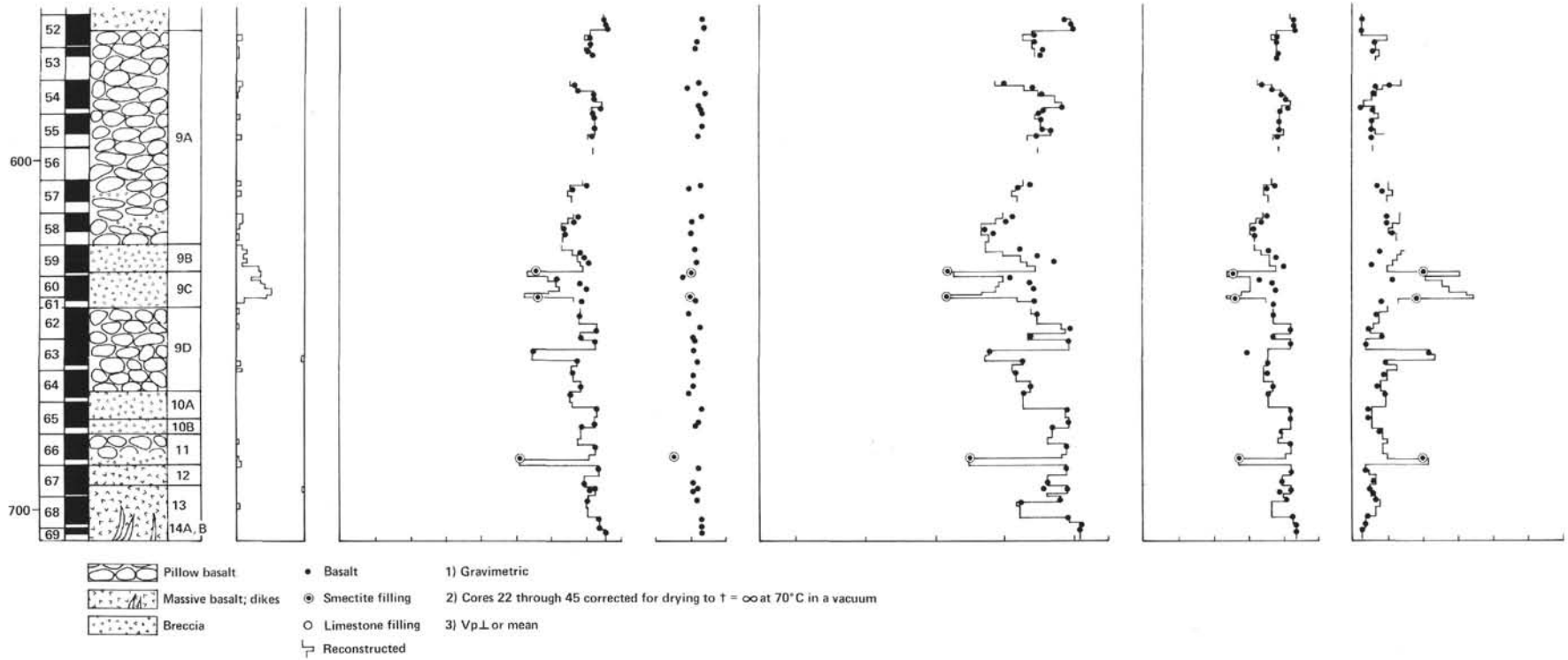

Figure 4. *Lithology, interstitial fillings, and physical properties versus depth in Hole 417D. All else the same as for Figure 3.*

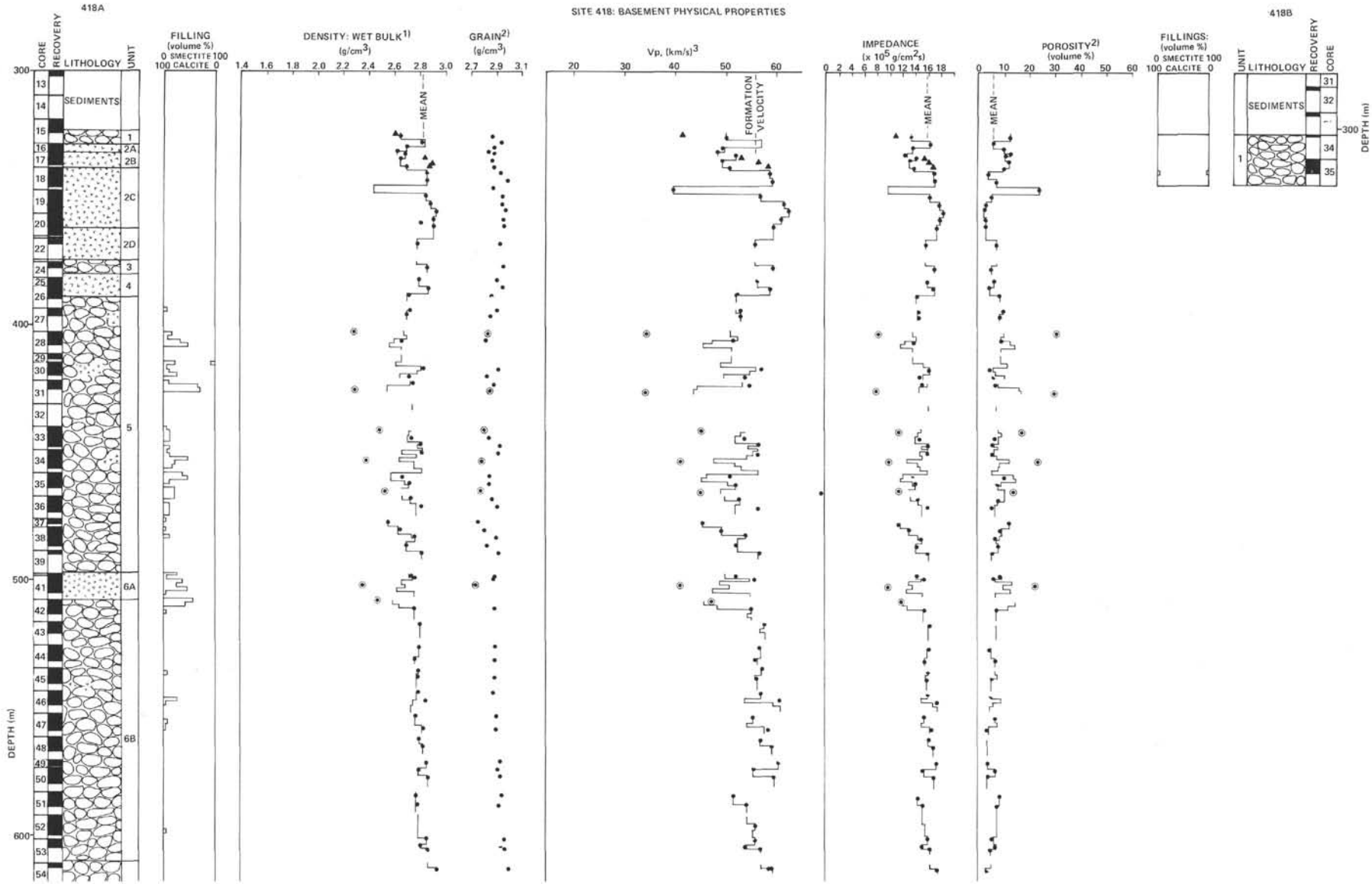

Figure 5. *Lithology, interstitial fillings, and physical properties versus depth in Holes 418A and 418B. All else the same as for Figure 3.*

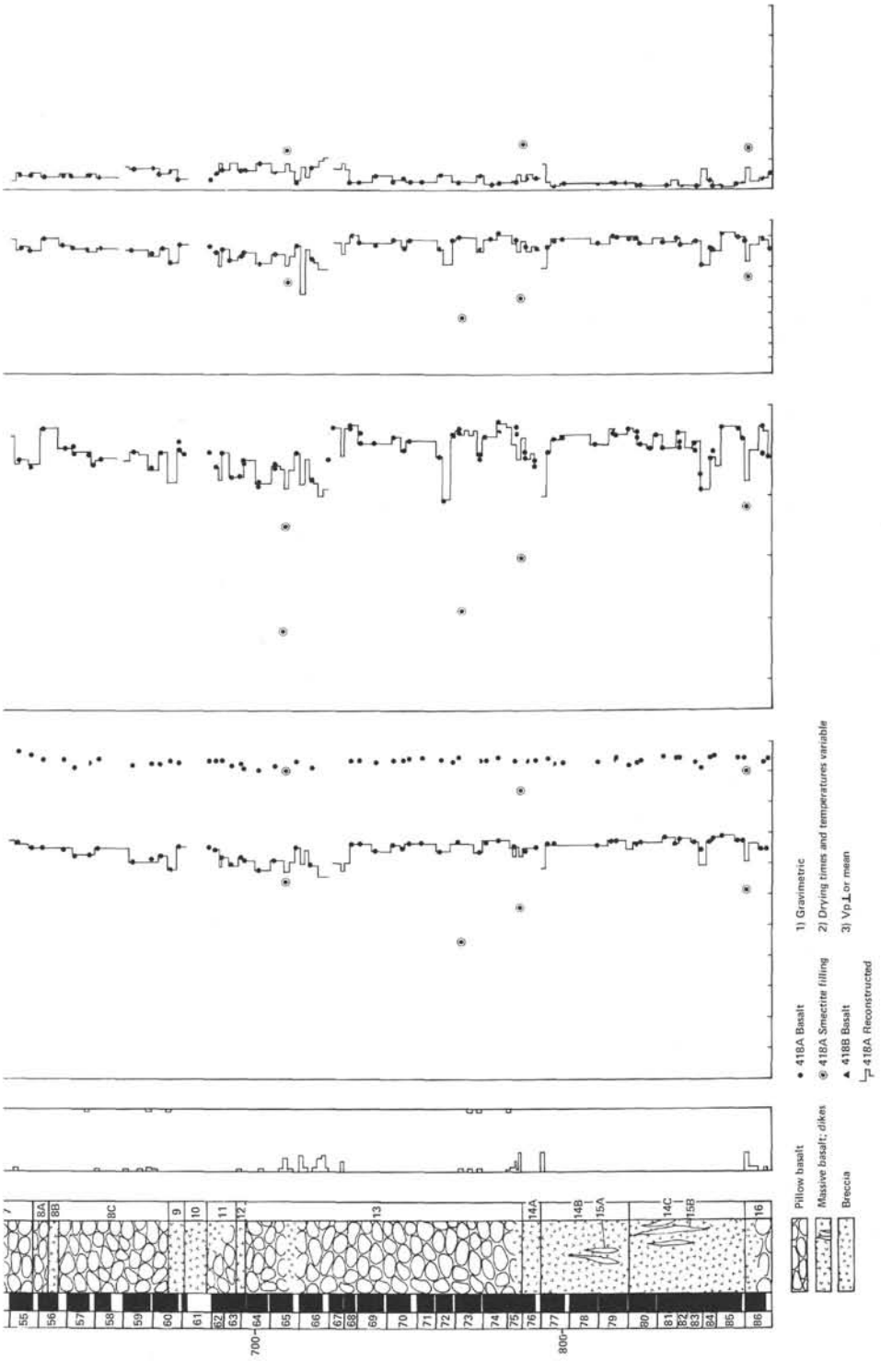

Figure 5. *(Continued).*

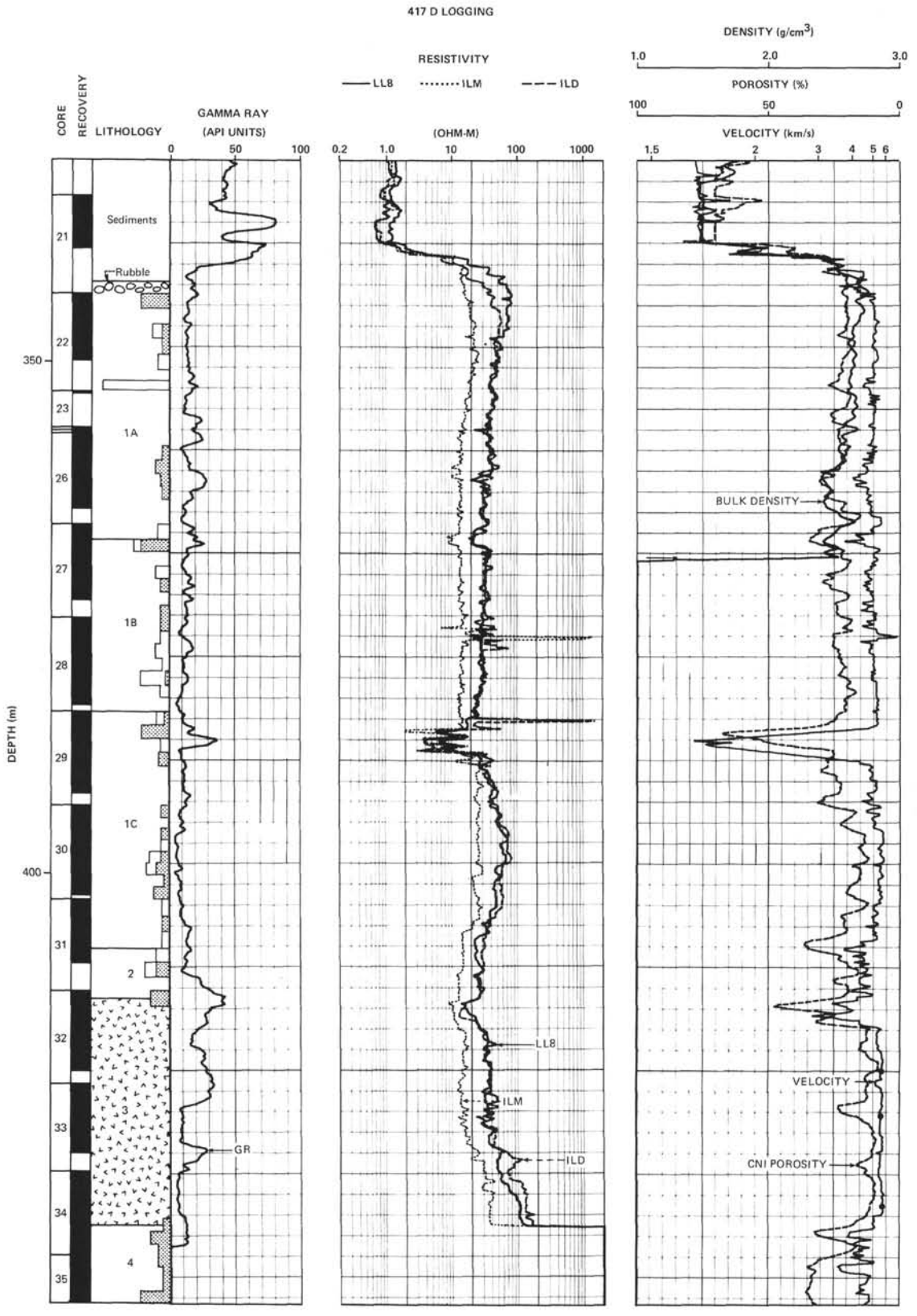

Figure 6. *Basement logging data and lithology versus depth in Hole 417D. Units 1, 2, and 4 are composed of pillow basalt, while Unit 3 (hachured) is composed of massive basalt; insets in lithology column represent abundance of limestone (plain) and smectite (light gray) on a scale of 0 per cent to 50 per cent; circles (•) on velocity curve in Unit 3 represent laboratory velocities (V_p) at an effective confining pressure of 0.1 kbar.*

TABLE 4
Sites 417 and 418 Average Physical Properties[a]

	Laboratory[b,c]		Synthetic[b]			
	Hole 417A	Holes 417D and 418A	Hole 417A	Hole 417D	Hole 418A	Hole 418B
Penetration (m)	209	910	209	366	544	10
Interstitial fillings (vol. %)	13.2	4.2	13.2[d]	5.7[e]	3.6[f]	1.5[g]
Wet bulk density, ρ (g/cm^3)	2.70 ±0.19 (N = 23)	2.79 ±0.13 (N = 185)	2.69	2.77	2.83	2.83
Grain density (g/cm^3)	2.94 ±0.03 (N = 21)	2.91 ±0.04 (N = 104)	–	–	–	–
Porosity (vol. %)	13.7 ±13.6 (N = 23)	8.4 ±5.5 (N = 104)	15.4	9.6	5.4	–
Velocity, V_P[h] (km/s)	4.99 ±0.79 (N = 23)	5.48 ±0.48 (N = 189)	4.68	5.35	5.58	5.31
Velocity, V_S[h] (km/s)	–	3.10 ±0.21 (N = 65)	–	–	–	–
Impedance, $V_P \times \rho$ ($\times 10^5$ g/cm^2-s)	13.6 ±2.8 (N = 23)	15.3 ±2.1 (N = 185)	12.6	14.8	15.8	15.0
Poisson's Ratio	–	0.28 ±0.01 (N = 65)	–	–	–	–
Electrical resistivity[h] (ohm-m)	–	120 (N = 48)	–	–	–	–
Air permeability (cm^2)	–	1.1×10^{-16} (N = 16)	–	–	–	–
Thermal conductivity (mcal/cm-s °C)	–	4.31 ±0.17 (N = 64)	–	–	–	–

[a] Assuming no large-scale cracks.
[b] Site 417 and 418 Reports (this volume).
[c] Hamano (this volume).
[d] Smectite.
[e] 5.0 per cent smectite and 0.7 per cent limestone.
[f] 3.5 per cent smectite and 0.1 per cent limestone.
[g] 0.8 per cent smectite and 0.7 per cent limestone.
[h] Samples water saturated, at room temperature and pressure.

417 and 418 on a scale of investigation typical of marine geophysical surveys.

THE OBLIQUE SEISMIC EXPERIMENT

As noted above and reported in detail by Stephen et al. (this volume), an oblique seismic experiment was conducted in Hole 417D to determine the velocity structure of the crust in the vicinity of the hole, to analyze the role of fissures and large cracks in determining the velocity of the crust, to look for anisotropy caused by cracks with a preferred orientation, and to measure crustal attenuation.

The experiment consisted of shooting explosive charges to a three-component geophone lowered into the hole from the *Glomar Challenger* (Figure 2). A cross pattern (Figure 7) with 12-km-long arms was fired with the geophone clamped 228 meters into the basement (571 m into the hole or 6060 m below the rig floor). The cross was oriented with its arms parallel and perpendicular to the magnetic lineations and thus, the original spreading axis in the area. A single 24-km-long line was then fired parallel to the spreading axis (south southwest-north northeast), with the geophone clamped 8 meters into the basement. The shooting was carried out by the *Virginia Key*, a research vessel from the Atlantic Oceanographic and Meterological Laboratories of the National Oceanic and Atmospheric Administration in Miami.

After processing to eliminate ship noise, the travel times and amplitudes were examined for evidence of anisotropy, attenuation, and topographic effects. The amplitude analysis (Figure 8) was carried out using the reflectivity synthetic seismogram method (Fuchs and Müller, 1971; Stephen, 1977). From the results of such analyses (e.g., Figure 9), it is clear that the velocity model which best reproduces the oblique seismic experiment data for Layer 2 at Site 417 is one with a uniform increase in compressional wave velocity from 4.8 km/s at the top of the basement to 6.4 km/s at a depth of 1.3 km and a similar increase in shear wave velocity from 2.6 to 3.6 km/s over the same interval.

Although fissures and large normal faults oriented parallel to the ridge have been observed in the axial zone on the Mid-Atlantic Ridge, no undisputed evidence for preferred crack orientation was found in Layer 2 at Site 417 from either velocity or amplitude studies. As can be seen in Table 6 (from Stephen et al., this volume), the mean north-south shear wave velocity (2.56 ±0.04 km/s) is not significantly different from the mean east-west velocity (2.66 ±0.14 km/s). In general, shear waves are well suited to the study of seismic anistropy since (a) the direct shear wave arrival plots as a straight line for about 3 km, whereas the direct compressional wave arrival falls on a curve; (b) shear wave

TABLE 5
Hole 417D Geophysical Logging Runs

Run	Tools	Scale of Investigation (m)	Interval Logged (m sub-bottom)	Data Quality	Remarks
1	High-Resolution Temperature (HRT)	–	0-44	Fair	Through pipe
			44-46	Fair	Open hole; terminated by caving
2	Borehole Compensated Velocity (BHC)	0.6	144-445	Excellent	Open hole
	Natural Gamma Ray	0.15	0-144	Fair	Through pipe
			144-445	Excellent	Open hole
	Caliper	–	–	Poor	Signal lead broken, spot readings only
3	Gamma Ray Density	0.15	320-369	Fair	Open hole
			144-443	Poor	Open hole; excentralizer broken; data not shown
	Neutron Porosity (CNL)	0.15	320-369	Fair	Open hole
			114-443	Poor	Open hole; excentralizer broken
	Natural Gamma Ray	0.15	114-443	Fair	Open hole
4	Electrical Resistivity				
	Induction Log Medium (ILM)	1.5	117-434	Fair	Open hole; no centralizer
	Induction Log Deep (ILD)	2.5	117-434	Excellent	Open hole; no centralizer
	Laterolog 8 (LL8)	1.0	117-434	Excellent	Open hole; no centralizer
	Natural Gamma Ray	0.15	117-434	Fair	Open hole

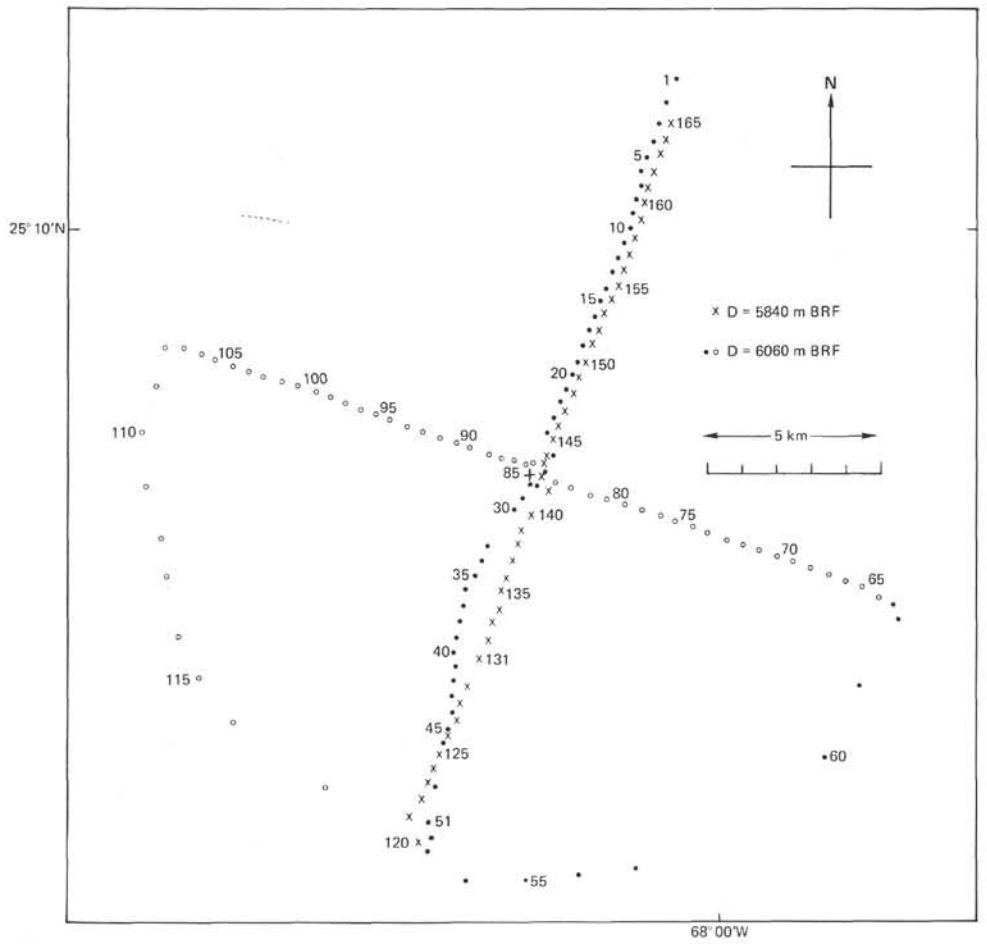

Figure 7. *Plan view of the oblique seismic experiment shooting pattern in the vicinity of Hole 417D (from Stephens et al., this volume). Plus (+) represents the position of the* Glomar Challenger; *the crosses (×) and circles (○) represent shots to the geophone in the 8- and 228-meter sub-basement positions, respectively. Magnetic lineations at Site 417 strike parallel to the south southwest-north northeast shooting line.*

amplitudes increase with range, in contrast to compressional wave amplitudes which decrease (Ergin, 1952); and (c) shear waves are theoretically more sensitive to the presence of water-filled cracks than compressional waves (Anderson et al., 1974). Since the present experiment was well suited to the detection of azimuthal anisotropy, it appears that large, oriented fissures are not present at Site 417.

The situation in Layer 3, however, is less clear. The average compressional wave velocities for the north-south and east-west lines are 6.71 ±0.30 km/s and 6.61 ±0.41 km/s, respectively, whereas the average shear wave velocities for the same lines are 3.77 ±0.10 km/s and 3.60 ±0.09 km/s, respectively. These values are not firm evidence of anisotropy in Layer 3, but if we assume that most of the spread in the errors is caused by small-scale topography and accept the mean values, then shear wave anisotropy on the order of 0.2 km/s may exist.

DATA COMPARISON

The scale of investigation of the three sets of data presented above ranges from approximately 10^{-2} meters for the laboratory data through 10^{0} meters for the logging data to about 10^{4} meters for the data collected by means of the oblique seismic experiment. Since all three types of data were obtained for Hole 417D, their comparison should make possible the determination of the volume fraction and scale of open cracks and fractures in the upper levels of the crust at Site 417. To this end, a summary of the porosity, density, velocity, and electrical resistivity data is presented in Table 7 for the interval in Hole 417D examined by all three techniques (Units 1-4). Also shown are summaries of the data for the pillow basalts of Unit 1A (for which all of the logging tools were working) and the relatively unfractured massive basalts at the base of Unit 3 which served as a calibration unit for the logging tools.

Several features of this table are remarkable. First, the average compressional wave velocity obtained by logging for the uppermost 100 meters of the crust (4.8 km/s for Units 1-4) is virtually identical to that obtained by the oblique seismic experiment, but both are considerably lower than the velocity derived for the same interval from laboratory data (5.3 km/s). This indicates that the crust is fractured on a scale larger than that of laboratory samples, but gener-

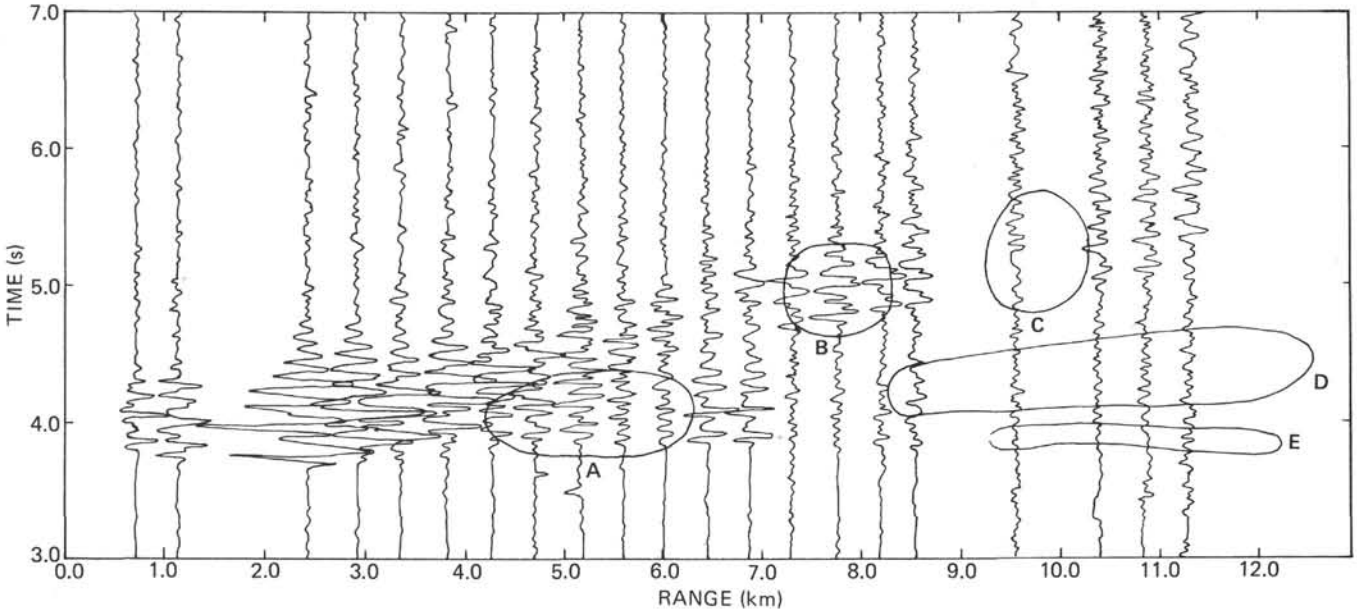

Figure 8. *Observed north-south horizontal component data from south line of oblique seismic experiment at Site 417; geophone 228 meters into basement (6060 m below rig floor); amplitudes weighted by (range/7.0)$^{2.9}$ for ranges greater than 7.0 km; time reduced to 6.0 km/s. Note signal character in regions A-E. Figure from Stephen et al. (this volume).*

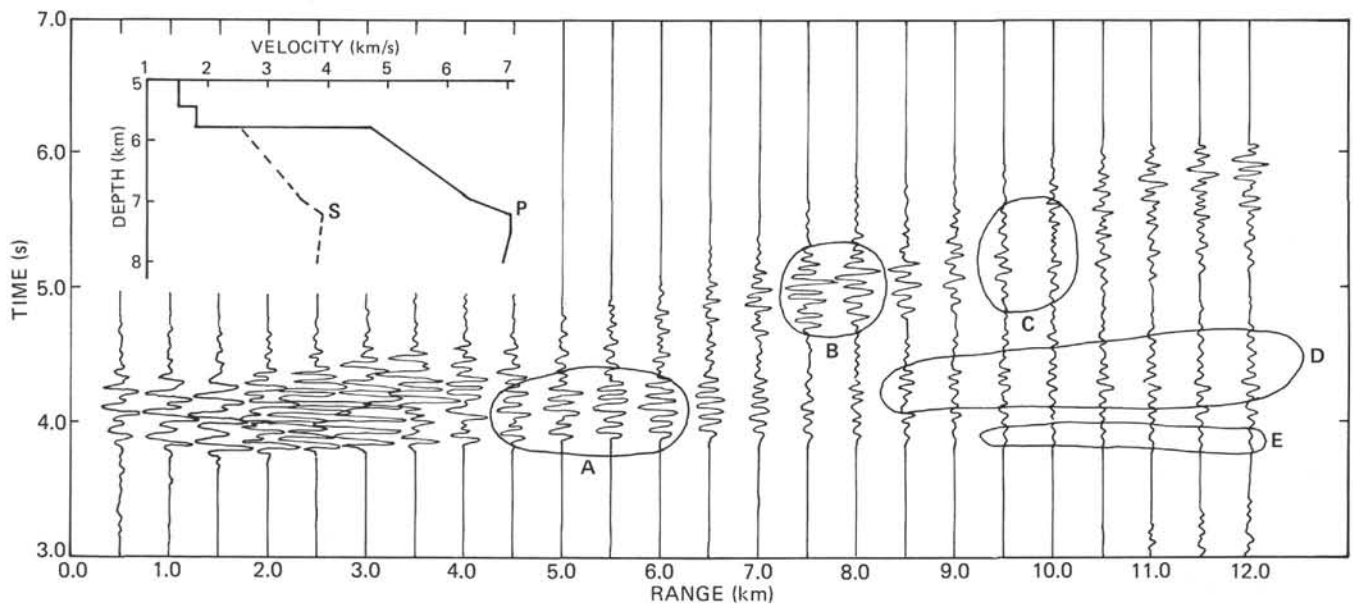

Figure 9. *Velocity model and resultant horizontal component synthetic seismogram representing best fit to salient features (regions A-E) of Figure 8. Velocity model represents compressional and shear wave velocity structure of crust at Site 417. Figure from Stephen et al. (this volume).*

ally less than the spacing between transmitter and receiver in the bore hole compensated velocity tool (0.6 m). Such spacing would be consistent with the cracks between individual pillows and the radial cracks within them.

Secondly, the average porosity of Unit 1A as determined by logging (13%) is about 5 per cent greater than the porosity determined from laboratory measurements (8.3%). This indicates that about 5 per cent of the formation by volume consists of open cracks, a value consistent with the 0.1 g/cm^3 discrepancy in density observed between laboratory and logging data in the same interval. Since the porosity tool measures porosity by determining the total amount of hydrogen in the formation, these cracks, like those between individual grains, are apparently filled with water.

Finally, it should be noted in Table 7 that the formation velocity determined by logging for Units 1 through 4 is

TABLE 6
Seismic Anisotropy at Site 417[a]

Shooting Line	Geophone Position (m below rig floor)	Layer 2 Shear Wave Velocity[b] (km/s)	Layer 3 Compressional Wave[c] Velocity (km/s)	Layer 3 Shear Wave Velocity[c] (km/s)
North	6060	2.49 ±0.02 (N = 5)	6.97 ±0.44 (N = 6)	3.75 ±0.12 (N = 11)
North	5840	2.48 ±0.04 (N = 6)	6.66 ±0.20 (N = 7)	3.88 ±0.02 (N = 6)
South	6060	2.61 ±0.05 (N = 4)	6.70 ±0.30 (N = 11)	3.63 ±0.08 (N = 8)
South	5840	2.67 ±0.04 (N = 3)	6.50 ±0.27 (N = 7)	3.81 ±0.19 (N = 5)
East	6060	2.72 ±0.21 (N = 4)	6.75 ±0.44 (N = 8)	3.68 ±0.11 (N = 6)
West	6060	2.60 ±0.01 (N = 4)	6.46 ±0.37 (N = 8)	3.51 ±0.06 (N = 7)
Mean		2.60 ±0.06	6.67 ±0.34	3.71 ±0.10

[a]From Stephen et al. (this volume).
[b]Direct.
[c]Refracted.

TABLE 7
Comparison of Laboratory, Logging, and Oblique Seismic Data in Hole 417D

	Unit 1A (pillow basalt)			Base of Unit 3 (unfractured massive basalt)			Units 1-4 (entire logged interval)		
Parameter	Laboratory[a] Results	Downhole Logging	Oblique Seismic Experiment	Laboratory[b] Results	Downhole Logging	Oblique Seismic Experiment	Laboratory[a] Results	Downhole Logging	Oblique Seismic Experiment
Density (g/cm^3)	2.79	2.7	–	2.88	–	–	2.78	–	–
Porosity (vol. %)	8.3	13	–	3.2	3	–	8.2	–	–
Velocity, V_p (km/s)	5.36 (5.6)	4.8	–	5.37 (5.87)	5.8	–	5.34 (5.6)	4.8	4.8
Resistivity (ohm-m)	74	40	–	–	120	–	97	35	–

[a]Density, porosity, and velocity data from synthetic profiles of Figure 4; values in parentheses are estimated velocities at 0.1 kbar effective confining pressure; resistivity data from Hamano (this volume).
[b]Measured values in Section 417D-34-2; velocity in parentheses measured at 0.1 kbar confining pressure.

identical to that of Unit 1A. We may thus be justified in extrapolating the conclusions drawn above for Unit 1A to the entire logged interval.

In order to understand the distribution of porosity within the logged interval, however, it is necessary to juxtapose the velocities determined by the three techniques as in Figure 10. There, the velocity profiles reconstructed from zero-pressure laboratory data, integrated logging transit times, and the results of the oblique seismic experiment are shown as a function of depth. Since the discrepancy between the logging and laboratory data is a measure of the volume fraction of cracks, Figure 10 suggests that the formation porosity associated with open cracks resides largely within the pillow basalts, while the massive basalts contribute relatively little to the porosity of the formation beyond their measured grain boundary porosity of about 3 per cent. Figure 10 also suggests that the breccias between flows often represent thin zones of very high crack porosity (up to 20% at the top of Unit 1C) in the crust. That the low velocities associated with the case noted here are not due to caving but to an aquifer of some antiquity is suggested by the high natural gamma-ray count seen at this level in Figure 6. It should be noted, incidentally, that in a rigorous comparison, laboratory velocities appropriate to *in situ* conditions would be used instead of the zero-pressure data shown in Figure 10. This procedure was not followed here because the velocity correction is variable (from 0.0 to 0.25 km/s, depending on density) and because the error in the estimate of porosity (2%), due to a maximum velocity correction of 0.25 km/s, is almost certainly less than the inaccuracy of the Wyllie relationship on which the estimate is based.

CONCLUSIONS

Since the beginning of the basement drilling program in 1974, approximately 1200 meters of basalt has been recovered in the Atlantic, of which 790 meters are from Sites

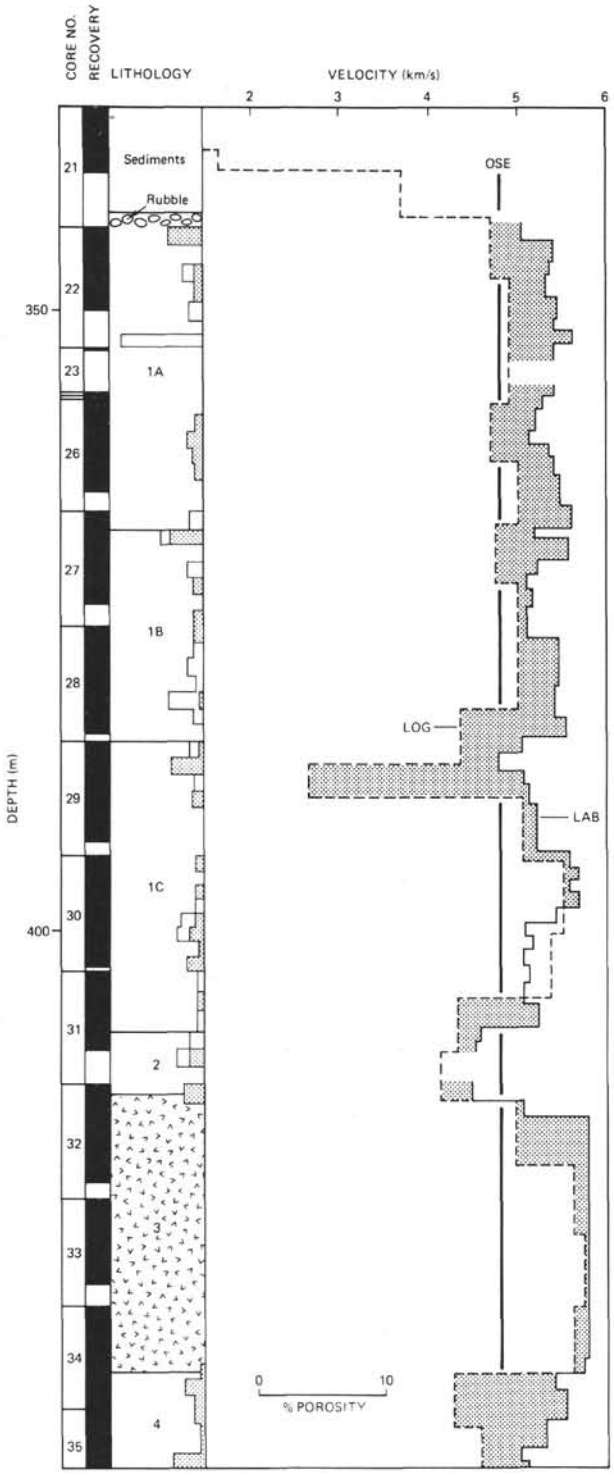

Figure 10. *Comparison of compressional wave velocities obtained from logging, physical properties studies, and the oblique seismic experiment in Hole 417D (see text). Discrepancy between laboratory and logging data (stippled area) is a measure of formation porosity due to open cracks. Units 1, 2, and 4 are composed of pillow basalts, while Unit 3 (hachured) is composed of massive basalt; insets in lithology column represent abundance of limestone (plain) and smectite (light gray) on a scale of 0 per cent to 50 per cent.*

417 and 418. If the sections drilled at these sites are representative of Cretaceous oceanic basement, it is clear that a number of important conclusions can be drawn from the results discussed above concerning the composition and physical state of the upper levels of Layer 2 in old oceanic crust.

1) *Composition:* The upper levels of the crust down to at least 0.5 km consist of about 90 per cent basalt, 5 per cent smectite, less than 1 per cent interpillow limestone, and 5 per cent open cracks filled with standing water. Of the basalts, 71 per cent consist of fractured pillow basalt, 22 per cent are relatively unfractured massive basalts, and 7 per cent consist of partially cemented basalt rubble. Dikes begin to appear at depths of 350 to 500 meters in the basement, but are not yet volumetrically significant.

2) *Internal structure:* Although the crust displays marked downhole variations in physical properties, it is unlikely that such variations will be detectable using surface geophysical techniques. It is possible, however, that the low velocity zones associated with breccias within the basement might be detected by deep-tow seismic reflection techniques.

3) *Resistivity:* The *in situ* electrical resistivity of the basement ranges from 3 ohm-meters in the breccias to about 200 ohm-meters in the massive basalts, with most values falling between 30 and 80 ohm-meters. Since the average laboratory resistivity of water-saturated basalts from the section is 97 ohm-meters and the resistivity of dry basalts at room temperature ranges from 10^3 to 10^6 ohm-meters, it is apparent that the basement is cracked and saturated with sea water having a low *in situ* resistivity (0.25 ohm-m at 21°C).

4) *Velocity:* Compressional wave velocities in the uppermost levels of the basement range for the most part between 4.7 and 5.3 km/s, with lower velocities displayed in breccias and velocities as high as 5.8 km/s in the massive basalts. The average formation velocity derived from both the oblique seismic experiment and integrated logging transit times is 4.8 km/s, a value consistent with those reported for Layer 2B by Houtz and Ewing (1976). This is considerably higher than the Layer 2A formation velocity of 3.6 km/s reported by Kirkpatrick (1978) for the basement section drilled in Hole 396B in young crust along the same flow line. It is consistent with the observation that Layer 2A does not commonly persist in the Atlantic beyond the 60-m.y. isochron. Examination of the core material from Hole 417D clearly indicates that the increase in formation velocity with age in the upper levels of Layer 2 is due to the infilling of cracks and interpillow voids by low-temperature alteration products such as calcite, smectite, and zeolite.

5) *Velocity versus depth:* Results of the oblique seismic experiment indicate that the compressional and shear wave velocities at Site 417 increase with depth, respectively, from 4.8 and 2.6 km/s at the top of Layer 2 to 6.4 and 3.6 km/s near its base. This could be due, in varying combinations, to decreasing alteration, to a decrease in cracks, or to changing mineralogy with depth. The laboratory velocities shown in Figure 11 suggest that the velocity gradient in Layer 2 can be explained in terms of the first two phenomena alone. These velocities increase with depth in response to decreasing alteration, reaching the velocity of fresh basalt (6.4 km/s) at a projected depth of about 700

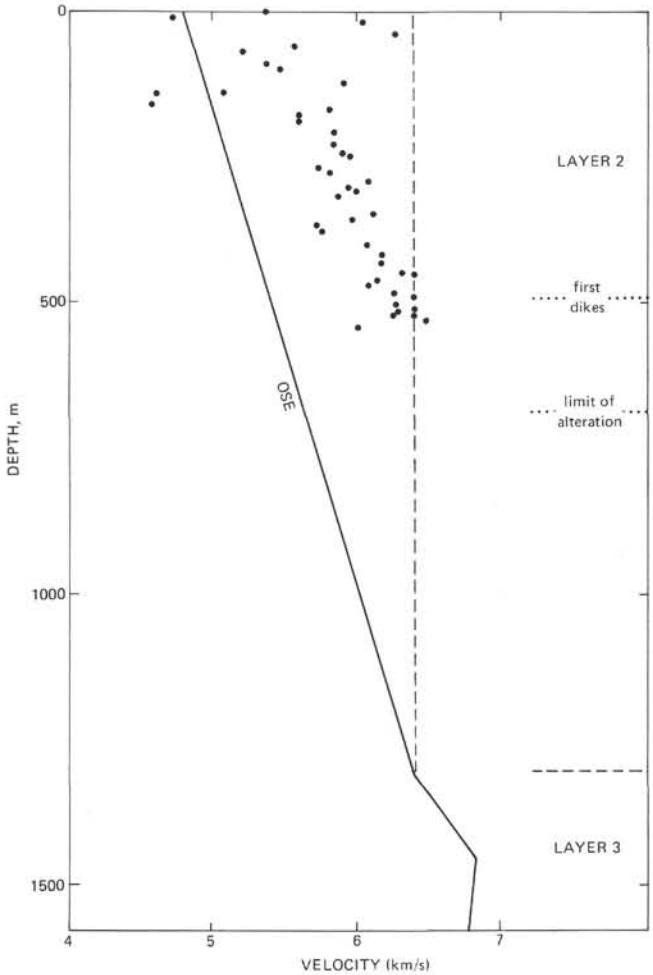

Figure 11. *Comparison of laboratory velocities of samples from Hole 418A (Christensen et al., this volume) and the results of the oblique seismic experiment in Hole 417D (Stephen et al., this volume). Laboratory velocities measured at an effective confining pressure of 0.1 kbar. Vertical dashed line represents velocity of fresh basalt at 1.0 kbar.*

meters, which would appear to be the maximum depth of alteration. The discrepancy between the laboratory and oblique seismic experiment data confirms that the crust is cracked, but the increase in the formation velocity with depth suggests that the cracks decrease with depth until the formation velocity reaches that of a fresh, crack-free basalt at the base of Layer 2. Since this velocity is still lower than that of Layer 3, the Layer 2/Layer 3 transition must be due to a change in mineralogy.

6) *Anisotropy:* We found no firm evidence of seismic anisotropy in Layer 2 from either velocity or amplitude analysis of the oblique seismic experiment data. Thus the large, open fissures observed parallel to the Mid-Atlantic Ridge in the floor of the median valley have either been filled with rubble and sediments or closed as they evolved into normal faults in the walls of the median valley. There is some weak evidence, however, of seismic anisotropy in Layer 3 with V_s slow by about 0.1 to 0.2 km/s parallel to the direction of spreading. Since open cracks cannot be postulated at this depth, this anisotropy may be due to the grain of sheeted dikes.

7) *Porosity, density, and permeability:* Although the crust at Sites 417 and 418 has experienced considerable infilling, the basement is strongly fractured *in situ*. The total porosity of the logged basement interval in Hole 417D ranges from 3 per cent in the massive basalts to as much as 20 per cent in the breccias, while the average for the pillow basalts and the logged interval as a whole is 13 per cent, of which about 8 per cent is due to grain boundary porosity in basalt and 5 per cent is due to open cracks filled with standing water. These cracks decrease the formation density by about 0.05 g/cm^3 to an average of 2.70 g/cm^3.

The most important influence of such cracks, however, is upon formation permeability. This can be estimated from the relation,

$$K = \frac{h^2 R_w}{4\pi S R} \tag{5}$$

where K is the permeability of the formation in darcies, h is the average crack width in centimeters, R_w is the resistivity of the interstitial water in ohm-meters, R is the average formation resistivity, and S is a shape factor close to unity (Scheidegger, 1960). Using the formation resistivity determined by logging (50 ohm-m), a sea-water resistivity of 0.25 ohm-meters, and an average crack width of 0.25 to 0.50 cm (estimated from the crack density and porosity of the formation), the permeability of the upper levels of the crust is found to range between 2500 and 10,000 darcies, in excellent agreement with the results of Johnson (this volume) from visual estimates of the density and distribution of cracks in the core. Such values imply that convective heat transfer in old oceanic crust is limited not by the permeability of the crust but by the availability of heat and the presence of overlying sediments and that the alteration of submarine basalts is only terminated by subduction.

ACKNOWLEDGMENTS

We wish to thank the Captains and crews of the *Glomar Challenger* and the *Virginia Key* for their assistance during the drilling, logging, and oblique seismic operations; Loic Beurdeley of Schlumberger, Ltd. for running the logging tools; R. Jones, J. Vohs, and S. Bearman for their assistance in processing the logging data; S. Blair, R. H. Wilkens, J. Hull, G. Bussod, and R. Prior for their assistance in the laboratory velocity studies; J. Kirkpatrick, K. E. Louden, and D. H. Matthews for their many helpful suggestions during the course of this study; and J. Orcutt for reviewing the manuscript. The laboratory velocity studies were supported by the Office of Naval Research Contract N-00014-75-C-0502.

REFERENCES

Anderson, D. L., Minster, B., and Cole, D., 1974. The effect of oriented cracks on seismic velocities, *J. Geophys. Res.*, v. 79, p. 4011-4016.

Aumento, F., Melson, W. G., et al., 1977a. Site 332. *In* Aumento, F., Melson, W. G., et al., *Initial Reports of the Deep Sea Drilling Project,* v. 37: Washington (U.S. Government Printing Office), p. 15-200.

_____, 1977b. Site 333. *In* Aumento, F., Melson, W. G., et al., *Initial Reports of the Deep Sea Drilling Project,* v. 37: Washington (U.S. Government Printing Office), p. 201-238.

Cann, J. R., Luyendyk, B., et al., 1979. Site 409. *In* Cann, J. R., Luyendyk, B., et al., *Initial Reports of the Deep Sea Drilling Project,* v. 49: Washington (U.S. Government Printing Office), p. 161-226.

Dmitriev, L., Heirtzler, J., et al., 1979. Holes 396A and 396B. *In* Dmitriev, L., Heirtzler, J., et al., *Initial Reports of the Deep Sea Drilling Project,* v. 46: Washington (U.S. Government Printing Office), p. 15-86.

Ergin, K., 1952. Energy ratio of the seismic waves reflected and refracted at a rock-water boundary, *Seism. Soc. Am. Bull.,* v. 42, p. 342-372.

Fuchs, K. and Müller, G., 1971. Computation of synthetic seismograms with the reflectivity method and comparison with observations, *Geophys. J. Roy. Astron. Soc.,* v. 23, p. 417-433.

Helmberger, D. V. and Morris, G. B., 1970. A travel time and amplitude interpretation of a marine refraction profile: transformed shear waves, *Seism. Soc. Am. Bull.,* v. 60, p. 593-600.

Houtz, R. and Ewing, J., 1976. Upper crustal structure as a function of plate age, *J. Geophys. Res.,* v. 81, p. 2490-2498.

Hussong, D. M., 1972. Detailed structural interpretation of the Pacific oceanic crust using ASPER and ocean bottom seismometer methods, Ph.D. thesis, University of Hawaii, Honolulu.

Hyndman, R. D. and Ade-Hall, J. M., 1974. Electrical resistivity of basalts from DSDP Leg 26. *In* Davies, T. A., Luyendyk, B. P., et al., *Initial Reports of the Deep Sea Drilling Project,* v. 26: Washington (U.S. Government Printing Office), p. 505-508.

Kirkpatrick, R. J., 1978. Results of down-hole geophysical logging Hole 396B, DSDP Leg 46. *In* Dmitriev, L., Heirtzler, J. et al., *Initial Reports of the Deep Sea Drilling Project,* v. 46: Washington (U.S. Government Printing Office), p. 401-408.

Melson, W. G., Rabinowitz, P. D., et al., 1979. Site 395: 23°N, Mid-Atlantic Ridge. *In* Melson, W. G., Rabinowitz, P. D., et al., *Initial Reports of the Deep Sea Drilling Project,* v. 45: Washington (U.S. Government Printing Office), p. 131-264.

Orcutt, J. A., Kennett, B. L. N., and Dorman, K. M., 1976. Structure of the East Pacific Rise from an ocean bottom seismometer survey, *Geophys. J. Roy. Astron. Soc.,* v. 45, p. 305-320.

Peterson, J. J., Fox, P. J., and Schreiber, E., 1974. Newfoundland ophiolites and the geology of the oceanic layer, *Nature,* v. 247, p. 194-196.

Raitt, R. W., 1963. The crustal rocks. *In* Hill, M. N. (Ed.), *The Sea:* New York (John Wiley), v. 3, p. 85-102.

Scheidegger, A. E., 1960. *The Physics of Flow Through Porous Media:* Toronto (University of Toronto Press).

Stephen, R. A., 1977. Synthetic seismograms for the case of the receiver within the reflectivity zone, *Geophys. J. Roy. Astron. Soc.,* v. 51, p. 169-181.

Spudich, P. K. P., Salisbury, M. H., and Orcutt, J. A., 1978. Ophiolites found in oceanic crust?, *Geophys. Res. Lett.,* v. 5, p. 341-344.

Wang, H. F. and Simmons, G., 1978. Microcracks in crystalline rocks from 5.2 km depth in the Michigan Basin, *J. Geophys. Res.,* v. 83, p. 5849-5856.